

Photochemical template removal and spatial patterning of zeolite MFI thin films using UV/ozone treatment

Qinghua Li ^a, Meri L. Amweg ^b, Chanel K. Yee ^b,
Alexandra Navrotsky ^{a,*}, Atul N. Parikh ^{b,*}

^a Thermochemistry Facility and NEAT ORU, University of California at Davis, Davis, CA 95616, USA

^b Department of Applied Science and NEAT ORU, University of California at Davis, Davis, CA 95616, USA

Received 9 March 2005; received in revised form 19 July 2005; accepted 20 July 2005

Available online 5 October 2005

Abstract

This paper describes an application of a non-thermal, photochemical calcination process for an efficient and spatially controlled removal of the organic structure-directing agent in the preparation of thin films of microporous or zeolite materials. We prepared thin-films of a high silica zeolite (structure code: MFI) following a previously published procedure. The films were illuminated using an ozone generating short-wavelength ultraviolet light in ambient environments and characterized using Fourier-transform infrared spectroscopy, imaging ellipsometry, thin-film X-ray diffraction, and scanning electron microscopy. Results presented here indicate that the UV/ozone treatment under nominally room temperature conditions leads to complete removal of template (structure-directing-agent) from zeolite films comparable to that achieved by thermal calcination. Furthermore, spatially addressing the UV/ozone illumination pattern using a physical mask resulted in the lateral confinement of the template removal from the zeolite film leaving behind a composite film composed of templated and template-free regions. Subsequent chemical treatment of the patterned film selectively removed the as-synthesized, unexposed, regions of the film thereby providing a means for the creation of isolated zeolite film islands at predetermined locations on the substrate surface.

© 2005 Elsevier Inc. All rights reserved.

Keywords: Microporous thin films; Calcination; Patterning; UV/ozone; Ellipsometric imaging

1. Introduction

Thin films of microporous materials or zeolites are attracting attention because of their potential usefulness in many technological applications including sensors, separation membranes for gases and liquids, low dielectric constant coatings, and as lasing media [1–5]. To this end, several synthetic approaches have recently emerged for the direct synthesis of zeolites on substrate surfaces as thin films. For instance, in situ crystallization [6,7]

seeded-growth [8,9] spin-coating of colloidal zeolite crystals [10], and vapor-transport methods [11] have all proved useful in the designed synthesis of microporous materials as thin films. Many of these zeolite films contain organic structure-directing-agents (SDA) which need to be removed. Most widely used template removal methods use high-temperature thermal calcination processes employing temperatures in the 300–550 °C range. However, the use of high-temperature calcination processes can induce significant thermal stresses especially at the substrate–film interface, further accentuated by the shrinkage of the zeolite framework which accompanies template removal. These stresses *can* result in defects and cracks within the film interior as well as at the interfaces [12–14]. Such stresses can become quite

* Corresponding authors. Tel.: +1 530 7547055; fax: +1 530 7522444 (A.N. Parikh).

E-mail addresses: anavrotsky@ucdavis.edu (A. Navrotsky), anparikh@ucdavis.edu (A.N. Parikh).

significant for thin films. Moreover, thermal calcination precludes the use of temperature-intolerant and organic/polymeric materials as substrates. Previous studies have shown that by using a carefully optimized calcination temperature program, crack-free thin films/membranes can be prepared, but such processes normally takes long calcination periods, and specialized sample pre-treatments [15]. Thus the processing cannot be easily generalized. Based on the above, generally applicable low temperature calcination methods for template removal from thin films are highly desirable.

Recently, we and others have shown that ozone-generating ultraviolet illumination provides a simple low-temperature alternative to the thermal calcination process for bulk microporous [16] and mesoporous materials [17,18] and their thin films [19,20]. While detailed mechanistic understanding of the process is still incomplete, it is generally believed that the process is photochemical. The simplest description of the overall process involves three overlapping photoinduced chemical reactions [16,21]. First, UV light with a wavelength below 245.4 nm (optimally at $\lambda = 184$ nm) facilitates the dissociation of oxygen (from the ambient) to produce ozone and atomic oxygen. Simultaneously, the 253.7 nm line emitted by the same lamp excites and/or dissociates the organic matrix, thereby producing activated species, such as ions, free radicals, and excited molecules. Finally, the activated organic species are readily attacked by atomic oxygen and ozone synergistically to form simpler volatile (or removable) products, such as CO_2 , H_2O , and N_2 which escape the sample interior. UV–ozone treatment is performed at room temperature under ambient air but local temperature at the substrate during the process often increases to 40–50 °C. By contrast, the currently used thermal calcination processes employ much higher temperatures (>500 °C). Thus, this nominally room temperature photochemical method may provide an efficient and simple method for the removal of organic SDA from zeolites and the formation of crack-free zeolite films/membranes. Furthermore, non-thermal calcination offers interesting opportunities to carry out calcination on thin films in a spatially controlled manner. It appears that by spatially addressing the photochemical calcination, it may be possible to create patterns of microporous material and functionality associated with it.

In the present work, high-quality silica zeolite MFI films were synthesized following a seeded-growth method. The organic templates were removed by both the thermal calcination and the photochemical, non-thermal calcination methods. The sample characteristics were compared using a combination of X-ray diffraction (XRD), Fourier-transform infrared spectroscopy (FT-IR), imaging ellipsometry and scanning electron microscopy (SEM) measurements. Spatial patterning was achieved by conducting the photochemical calcination

in conjunction with a mask and subsequent gentle chemical treatment was shown to enhance the patterns by selective removal of the SDA-containing regions of the patterned MFI thin films.

2. Experimental section

2.1. Preparation of MFI thin films

A previously established seeding method [9] was used for the preparation of MFI zeolite films. Briefly, seed crystals of TPA-silicalite-1 with an average size of ~ 60 nm were first adsorbed on charge-reversed single crystal silicon (100) substrates. TPA-silicalite-1 (MFI) films were subsequently grown by a hydrothermal treatment of the above seeded silicon substrate in a precursor solution at 100 °C for approximately 24 h. The precursor solution comprised the molecular constituents in a predetermined molar composition of $3\text{TPAOH}:25\text{SiO}_2:1300\text{H}_2\text{O}:100\text{EtOH}$ where TPAOH is tetrapropylammonium-hydroxide and EtOH is ethanol. The silica source was from tetraethylorthosilicate (TEOS). Subsequently, the samples were rinsed with a 0.1 M ammonia solution to remove sediments and any excess unreacted gel from the film surface.

2.2. Removal of SDA from as-synthesized MFI films

Each as-synthesized MFI sample was cut into two pieces to enable thermal and non-thermal calcination on single films. One piece was exposed to ozone-generating short-wavelength ultraviolet (UV) light ($\lambda = 184\text{--}257$ nm), produced by a low- or medium-pressure Hg discharge lamp ($10\text{--}20$ mW cm^{-2} UVP, Inc., Upland, CA) in a quartz envelope. The lamp is maintained in a closed chamber under ambient laboratory conditions. The sample was placed in the UV/ozone reactor so that the substrates were about 2–3 mm away from the light source. The exposure period of ~ 4 h was used, however the exposure periods were not optimized. The second piece was calcined at 550 °C for 6 h using a heating rate of 0.2 °C/min and a cooling rate of 0.3 °C/min. Total calcination time in the thermal treatment is more than 3 days.

Spatially directed UV illumination was achieved by carrying out the UV-treatment in conjunction with a physical mask. This mask, comprising alternating features of chrome deposited on quartz, was produced using standard photolithography techniques. The masks were fabricated either at the Northern California Nanotechnology Center at UC Davis or were purchased from Photoscience, Inc. (Torrance, CA). Subsequent chemical treatment of selected patterned samples was performed by immersing the samples in 0.2 N NaOH for fixed incubation periods.

2.3. Characterization

Prior to and after UV treatment or thermal calcination, XRD-data were collected with an Inel X-ray diffractometer (XRG 3000) using Ni-filtered CuK α radiation and operated at 30 kV and 30 mA. The film surface was oriented perpendicular to a plane defined by the X-ray source, sample holder and detector. The step size was 0.01° and the time per step was 80 s.

FT-IR spectra were obtained in a reflection mode using a IRscope II (Bruker, Göttingen, Germany) connected to a Bruker Equinox 55 FT-IR spectrophotometer (Bruker, Göttingen, Germany) equipped with a liquid nitrogen cooled MCT detector and a motorized X–Y stage manipulator. Measurements of specific regions (grid area or square area) on samples were aided with a 3D video-assisted measurement software and a CCD camera. The mid-IR spectra in the frequency range of 4000–600 cm⁻¹ were obtained at a 4 cm⁻¹ resolution for 500 scans using a Blackman Harris 3 term apodization. Both the microscope and the spectrometer were purged with dry and carbon dioxide-free air. The data analysis was performed using Grams 32 (Galactic Industries, Salem, NH) software.

The film morphology and thickness were determined by analysis with a Philips XL 30 SEM equipped with a LaB₆ emission source. The samples for SEM were sputtered with a thin carbon layer prior to the measurements. Imaging ellipsometry measurements were performed using a commercial iElli2000 (Nanofilm Technologie, Göttingen, Germany) operating at 532 nm using a frequency-doubled Nd:YAG laser (adjustable power up to 20 mW) and equipped with a motorized goniometer for an accurate selection of the incidence angle. The ellipsometer employed the typical polarizer–compensator–sample–analyzer (PCSA) nulling-configuration in which a linear polarizer (P) and a quarter-wave plate (C) yields an elliptically polarized incident beam. Upon reflection from the sample (S), the beam is gathered via an analyzer (A) and imaged onto a CCD camera through a long working distance CF plan 10 \times (NA:0.35, Nikon, Japan) objective. The P, C, and A positions that yielded the null condition are then converted to the ellipsometric angles, delta and psi. Measurements were taken at an incidence angle of 60°. Thicknesses were estimated from the ellipsometric angles using a computer-aided modeling program based on Fresnel reflections. Refractive indices were assumed to be 4.1502–0.0449i and 1.4–0.0i for silicon and the zeolite films, respectively.

3. Results and discussion

The nominally room temperature photochemical calcination (UV-treatment) exposes the sample films to a

freshly-cleaned UV lamp-grid with samples maintained 2–3 mm below the lamp surface. The exposure time, 3–6 h, required for complete removal of the SDA and its decomposition products, was found to depend on the lamp power, cleanliness of the lamp, presence of added oxygen, and the distance of the sample from the lamp as well as the thickness of the zeolite film. FT-IR measurement shows that the 4 h exposure is adequate in our UV exposure configuration to fully remove SDA from MFI thin film.

SEM images shown in Fig. 1(a) and (b) represent the top- and side-view images of as-synthesized MFI films grown on a seeded silicon wafer. The images reveal the formation of a continuous film displaying densely packed crystals with a smooth surface and appears to be free of significant cracks and pin-holes. The lateral dimensions of the crystals at the surface appears to be about 100 nm with many crystals that have grown as large as 150–200 nm, suggesting fusion and growth of initial seed crystals during the hydrothermal treatment. The side-view images suggest the film thickness to be approximately 440 nm. These values are in good agreement with previous results [17]. Corresponding SEM images of photochemically and thermally calcined samples are shown in Fig. 1(c)–(f). The images confirm that neither calcination treatment used here gave rise to any significant changes in the film morphology. Subtle changes in film thicknesses were revealed by the ellipsometric data. These data estimate that the thickness of as-synthesized film is approximately 460 nm, while after the removal of SDA by UV–ozone or thermal processes, the thickness of the film reduces to ~420 nm. Furthermore, the SEM data did not reveal any significant cracks or defects in the calcination treatments used in the present study.

The evidence for the removal of organic SDA was furnished by FT-IR spectroscopy. FT-IR spectra of as-synthesized and thermally calcined samples are shown in Fig. 2. The dashed traces in Fig. 2 show the high frequency region (2700–3100 cm⁻¹) of the spectra. The trace for as-synthesized samples is characterized by the presence of a number of overlapping peaks with peak-maxima at 2973, 2966, 2939, and 2876 cm⁻¹, which are straightforwardly assigned to the methylene (–CH₂) and methyl (–CH₃) C–H stretching vibrations [22]. Lower frequency regions of the spectra could not be easily resolved presumably because of low signal throughput obtained in the microscopy geometry. By contrast, in the UV–ozone treated and thermally calcined samples, these peaks are noticeably absent (vanishing below the noise level in our spectra), confirming the essentially complete removal (residual organics well below 1% original content) of the SDA. We further note that the spectra in Fig. 2 appear to suggest that under the conditions employed in the present study, NTC appeared even more efficient for the template removal. Taken

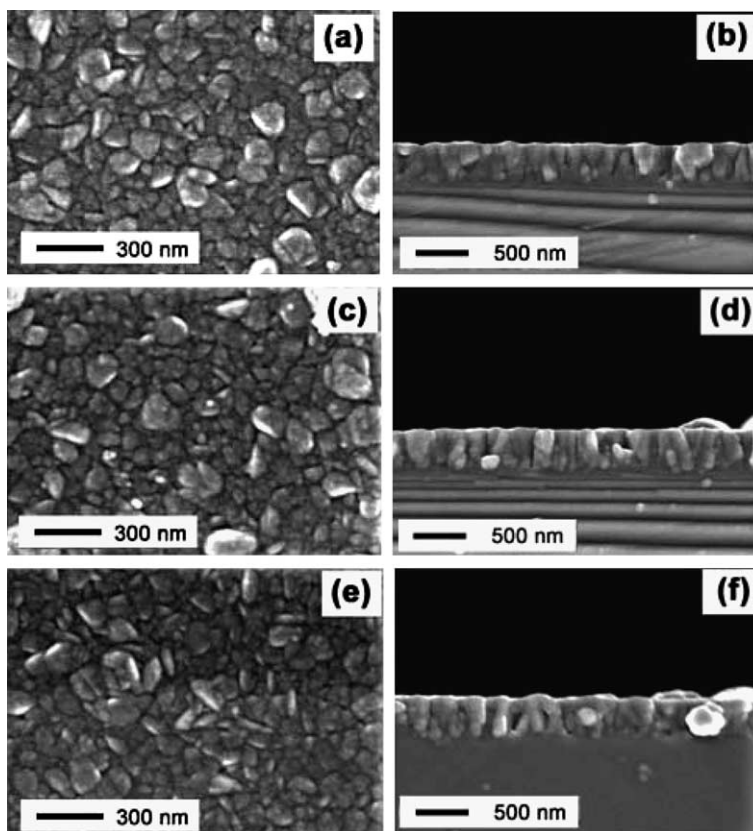


Fig. 1. SEM micrographs of the films. Top- and side-view images of the as-synthesized film (a, b), top- and side-view images of the UV-exposed film (c, d), and top- and side-view images of the calcined film (e, f).

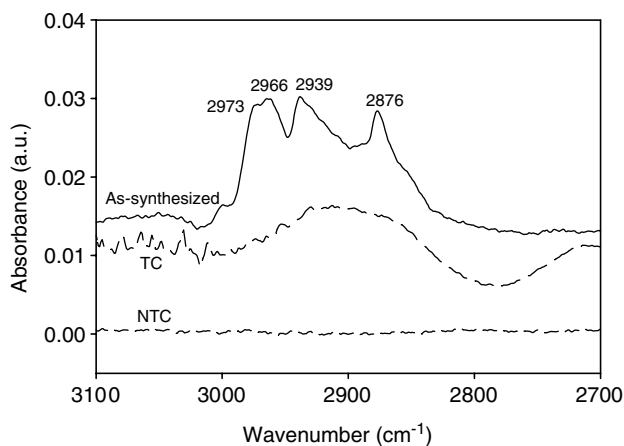


Fig. 2. FT-IR traces in the high frequency mid-infrared regions ($2700\text{--}3100\text{ cm}^{-1}$) for the as-synthesized and the UV-exposed (square) MFI thin film.

together, these results are in excellent correspondence with our earlier results wherein MFI bulk powder was shown to lose all measurable template upon photo- and thermal-calcinations [16].

Additional evidence for the removal of SDA by UV exposure is provided by thin film XRD. The diffractograms shown in Fig. 3 (panels a–c) represent the XRD

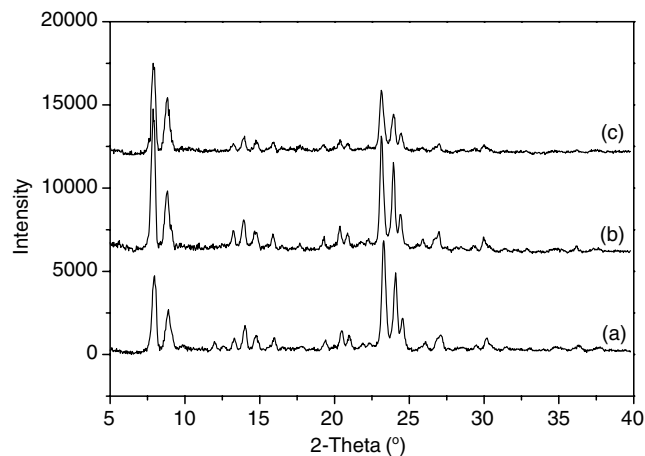


Fig. 3. XRD patterns of the as-synthesized film (a), the UV-exposed film (b) and the calcined film (c).

patterns obtained for the as-synthesized film, the UV-ozone treated film and the thermally calcined film, respectively. Strong XRD peaks of the supporting layer at 56.2° ((001) oriented silicon wafer) in the supported MFI zeolite film (not shown in the figure) and randomly oriented pattern indicate that the coated MFI zeolite film is thin, as confirmed by SEM images. The XRD pattern of the as-synthesized thin film shows that the

intensities of the first two lines at about 7.9° and 8.8° 2θ are lowered due to the presence of SDA in the intracrystalline voids (see Fig. 3(a)). When the sample is treated by UV exposure or thermal calcinations, the relative intensity changes, i.e., the first two lines relatively increased in intensity whereas the lines at about 11.9° and 12.5° 2θ decreased in intensity, as shown in Fig. 3(b) and (c). These intensity changes can be explained as the expected consequence of a decrease in loading, i.e., removal of extra framework organic (SDA) and inorganic species incorporated into the structural voids during synthesis [23]. Note also that the intensity increase for the NTC samples in Fig. 3 are more pronounced than for TC samples, further confirming that under the conditions employed, NTC appeared more efficient for surfactant removal than TC.

Taken together, the experimental evidence above confirms that the photochemical calcination using ozone generating UV light provides an alternative to thermal calcination for zeolitic thin films. Our results suggest that all features of the thermal calcination (1) near-complete template removal, (2) the retention of the inorganic framework, and (3) film morphology attributes are achieved using the nominally room temperature photochemical calcination process.

Conventionally, zeolite films must be carefully treated with temperature-programmed calcination process to avoid the formation of crack, especially for thin films. The total calcination time of thin film used in such treatments is often more than 3 days, under high temperature (550°C) conditions. By contrast, the UV-treated method occurs at low temperature ($<50^\circ\text{C}$) conditions, and the total calcination time for the removal of SDA is dramatically shortened (from 3 days to 4 h). This may provide a more efficient and economical way to prepare high-quality zeolite films/membranes. Crack-free thin MFI zeolite membranes treated by UV exposure will be applied in permeation and flux tests in the future.

An attractive feature of the UV–ozone template removal method is the ability to pattern zeolite thin films, which has many potential applications in sensor microarrays, catalyst screening, and nanochemistry. Patterns as small as $25\ \mu\text{m}$ was used to mask as-synthesized MFI thin film. After UV exposure for 4 h, optical patterns are easily observed using an imaging ellipsometer, as shown in Fig. 4(a). The brighter square region indicates regions of the sample that received direct UV exposure, while the darker grid region reflects samples areas that remained protected from the UV illumination. Optical contrast derives from the thickness decrease and/or index of refraction change between the exposed and unexposed region due to template removal and/or structure condensation. Fig. 4(b) shows FT-IR spectra of UV-exposed (square) and UV-unexposed (grid) areas. These data show that the characteristic peaks in the CH stretching frequency range (2800 –

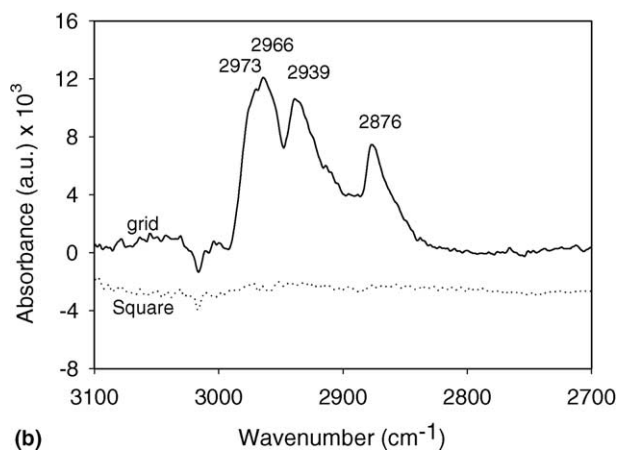
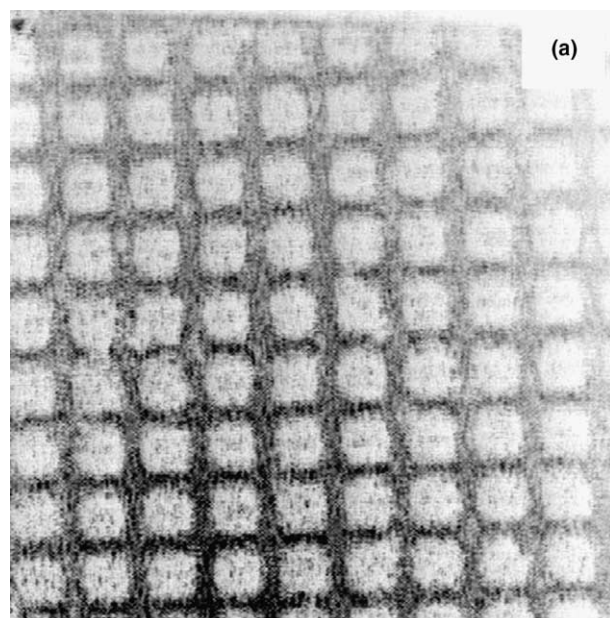


Fig. 4. Optical microscope image of patterned thin film (a) showing contrast between UV-exposed region (brighter square) and UV-unexposed region (darker grid). The square features were $25\ \mu\text{m}$ in linear dimensions. (b) FT-IR traces in the high frequency mid-infrared regions (2700 – $3100\ \text{cm}^{-1}$) for the UV-exposed (square) and UV-protected (grid) regions of a photochemically patterned MFI thin film.

$3000\ \text{cm}^{-1}$) are readily observed in the grid areas, while these peaks are absent in the square regions of the sample. These results indicate that the template is removed selectively only from the UV exposed parts of the sample, confirming the patternability of the photochemical template removal process.

Following the UV exposure, subsequent chemical processing of the films can be used to enhance the observed patterns through preferential etching of the UV-unexposed (grid) regions of the samples. The patterned film was immersed in an aqueous $0.2\ \text{N}$ NaOH solution. At various times the sample was removed from the solution and examined for the variations in optical contrasts using imaging ellipsometry. These data are shown in Fig. 5. With the increase in exposure time to

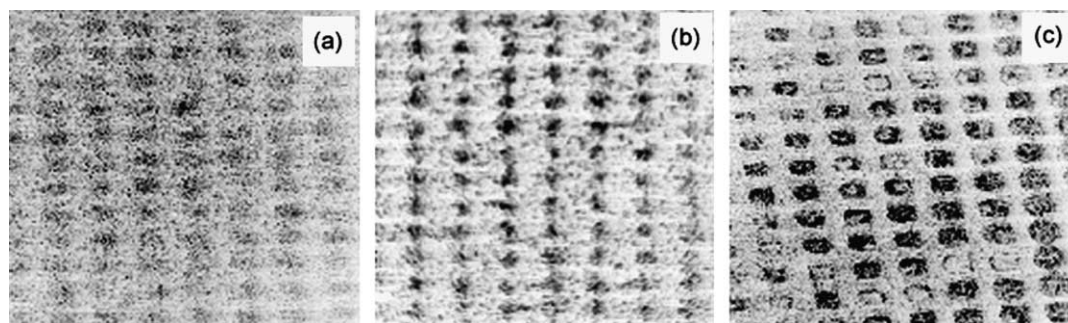


Fig. 5. Ellipsometric images of patterned films immersed in a 0.2 N NaOH solution for three different incubation periods: (a) 10 min, (b) 30 min, (c) 80 min.

the NaOH solution, the optical contrast gradually reversed as the thickness of the UV unexposed regions diminished from above that of the exposed parts to nearly zero. This indicates the grid part is preferentially removed relative to the square one. Thus, patterned islands of MFI thin films result as an end point in which the as-synthesized film region containing SDA is completely removed, while the UV-exposed film region without SDA remains. More details are being investigated in our laboratories.

4. Conclusion

In summary, a nominally room temperature, UV/ozone treated method is shown to provide a useful alternative to the high-temperature thermal calcination methods. This method provides an efficient and rapid approach for the removal of template from zeolite thin films under near room temperature conditions while retaining the inorganic framework. Because of low temperature used in the photochemical process, the formation of cracks and defects, such as may be caused by the different expansion between the zeolite and the support *in thin films* during thermal calcination process, can be minimized, thereby allowing the design of low defect films and membranes. In addition, the photochemical calcination offers a new patterning capability as demonstrated here. Spatially directed UV exposure on zeolite thin films for selective removal of template from films was shown to result in template-loaded and template-free microporous regions within a single contiguous thin film sample. We envisage such composite structures to be useful to direct microporosity associated functionality to specific regions of the sample and allow direct comparison of the roles of templates on zeolite film properties. Moreover, UV-patterned zeolite thin films when subjected to subsequent simple chemical treatments was found to allow the creation of patterned islands of zeolite thin films. The method appears general and may be useful in the design of multifunctional elec-

tronic, optical, catalytic and sensing platforms using microporous thin films.

Acknowledgment

This work received support from the National Science Foundation (Grant #DMR01-01391). A.N.P., M.L.A., and C.K.Y. acknowledges support through a grant from the Office of Science, US Department of Energy (DE-FG02-04ER46173).

References

- [1] M.E. Davis, *Nature* 417 (2003) 813.
- [2] K.J. Balkus Jr., L.J. Scollie, S.J. Riley, B.E. Gnade, *Thin Solid Films* 260 (1995) 4.
- [3] T. Bein, *Chem. Mater.* 8 (1996) 1636.
- [4] N. Nishiyama, K. Ueyama, M. Matsukata, *Micropor. Mater.* 7 (1996) 299.
- [5] Z. Shan, W.E.J. van Kooten, O.L. Oudshoorn, J.C. Jansen, H. van Bekkum, *Micropor. Mesopor. Mater.* 34 (2000) 23.
- [6] E.R. Geus, M.J. den Exter, H.J. van Bekkum, *Chem. Soc., Faraday Trans.* 88 (1992) 3101.
- [7] Z. Wang, Y. Yan, *Chem. Mater.* 13 (2001) 1101.
- [8] L. Boudreau, M. Tsapatsis, *Chem. Mater.* 9 (1997) 1705.
- [9] J. Hedlund, S. Mintova, J. Sterte, *Micropor. Mesopor. Mater.* 28 (1999) 185.
- [10] S. Mintova, T. Bein, *Adv. Mater.* 13 (2001) 1880.
- [11] E. Kikuchi, K. Yamashita, S. Hiromoto, K. Ueyama, M. Matsukata, *Micropor. Mater.* 11 (1997) 107.
- [12] K. Wegner, J. Dong, Y.S. Lin, *J. Membr. Sci.* 158 (1999) 17.
- [13] E.R. Geus, H. van Bekkum, *Zeolites* 15 (1995) 333.
- [14] J. Dong, Y.S. Lin, M. Hu, R.A. Peascoe, E. Andrew Payzant, *Micropor. Mesopor. Mater.* 34 (2000) 241.
- [15] J. Hedlund, J. Sterte, M. Anthonis, A. Bons, B. Carstensen, N. Corcoran, D. Cox, H. Deckman, W. Gijst, P. de Moor, F. Lai, J. McHenry, W. Mortier, J. Reinoso, J. Peters, *Micropor. Mesopor. Mater.* 52 (2002) 179.
- [16] A.N. Parikh, A. Navrotsky, Q. Li, C.K. Yee, M.L. Amweg, *Micropor. Mesopor. Mater.* 76 (2004) 17.
- [17] M.T.J. Keene, R. Denoyel, P.L. Llewellyn, *Chem. Commun.* (1998) 2203.
- [18] M.T.J. Keene, R.D.M. Gougeon, R. Denoyel, R.K. Harris, J. Rouquerol, P.L.J. Llewellyn, *Mater. Chem.* 9 (1999) 2843.

- [19] T. Clark, J.D. Ruiz, H. Fan, J. Brinker, B.I. Swanson, A.N. Parikh, *Chem. Mater.* 12 (2000) 3879.
- [20] A.M. Dattelbaum, M.L. Amweg, L.E. Ecke, C.K. Yee, A.P. Shreve, A.N. Parikh, *NanoLetters* 3 (2003) 719.
- [21] J.R. Vig, *J. Vac. Sci. Technol. A* 3 (1985) 1027.
- [22] L.J. Bellamy, *The Infrared Spectra of Complex Molecules*, Chapman and Hall, London, 1975, pp. 374–383.
- [23] E.L. Wu, S.L. Lawton, D.H. Oison, A.C. Rohrman Jr., G.T. Kokotailo, *J. Phys. Chem.* 83 (21) (1979) 2777.